

## A comparison of satellite and reanalysis precipitable water products over the Maritime Continent using GNSS-derived precipitable water

**Last Modified:** 16<sup>th</sup> Dec, 2019

**Acknowledgements:** Thanks goes to Professor Zhiming Kuang for inspiring this project and for his patience while I juggle multiple courses over the semester. Many thanks also goes to the Julia community for their patience and their help as I learn a new coding language.

### Abstract

In this project I compare the MIMIC-TPW2m satellite and ERA5 reanalysis precipitable water products using GNSS-derived precipitable water as the ground truth. Despite the fact that ERA5 is the product of reanalysis model output, it is closer to GNSS-derived precipitable water values than MIMIC-TPW2m. We postulate that this due to the fact that MIMIC-TPW2m algorithms do not work well over land as compared to the ocean, and therefore reanalysis datasets are still valuable in helping us characterize the climatology of precipitable water vapour over the Maritime Continent. Future studies using precipitable water data should keep this in mind.

### Introduction

The variability of precipitation and humidity play important roles in the Maritime Continent [Ramage, 1968, Yamanaka, 2016], but the complex interaction between land and sea within the region is hard to represent even in the most recent state-of-the-art climate models due to the spatial resolution needed to explicitly represent convection over a region which consists of many thousands of incredibly small islands [Neale and Slingo, 2003, Love et al., 2011, Jourdain et al., 2013]. However, the Maritime Continent is one of the most prominent sources of global latent heat in the atmospheric circulation, and model biases of precipitation and therefore latent heat flux in the Maritime Continent show up in numerous teleconnection errors all the way to the extratropics [Neale and Slingo, 2003, Wang et al., 2014].

But to improve representation of the Maritime Continent in our models, we first need to understand the climate processes that occur in the Maritime Continent and how the interaction between land and sea modulates these processes. Yet, our understanding still remains relatively limited even for how the Madden-Julian Oscillation [Madden and Julian, 1994], which is the dominant mode of intraseasonal climatic variability within the tropics, interacts with the Maritime Continent [Rui and Wang, 1990, Ling et al., 2019b,a]. For example, some have suggested

that the strong diurnal cycle of rainfall and convection over the Maritime Continent acts as a “Barrier Effect” on the Madden-Julian Oscillation that can prevent it from propagating over the region [Neale and Slingo, 2003, Wang and Sobel, 2017, Ling et al., 2019a]. However, it is not the only theory, and many other explanations abound that can reasonably explain this phenomenon [Rui and Wang, 1990, Inness and Slingo, 2006, Wu and Hsu, 2009, Ling et al., 2019b,a].

This understanding can be achieved using a combination of both observations and a hierarchy of models, with models used to test and validate the theories we proposed based on our observations. Here, I focus on building an understanding of the Maritime Continent precipitation and precipitable water climatology based on some of the latest satellite datasets with near-global coverage, specifically the Global Precipitation Mission IMERG precipitation data [Hou et al., 2014, Huffman et al., 2019] the Morphed Integrated Microwave Imagery at CIMSS (MIMIC)-TPW2m precipitable water data, and the new-generation ERA5 reanalysis dataset that also incorporates satellite data. As a way to validate the MIMIC-TPW2m and ERA5 datasets, I both datasets with GNSS-derived values of precipitable water. We are able to do this because GNSS data retrieval, unlike microwave satellite data, is independent on the re-

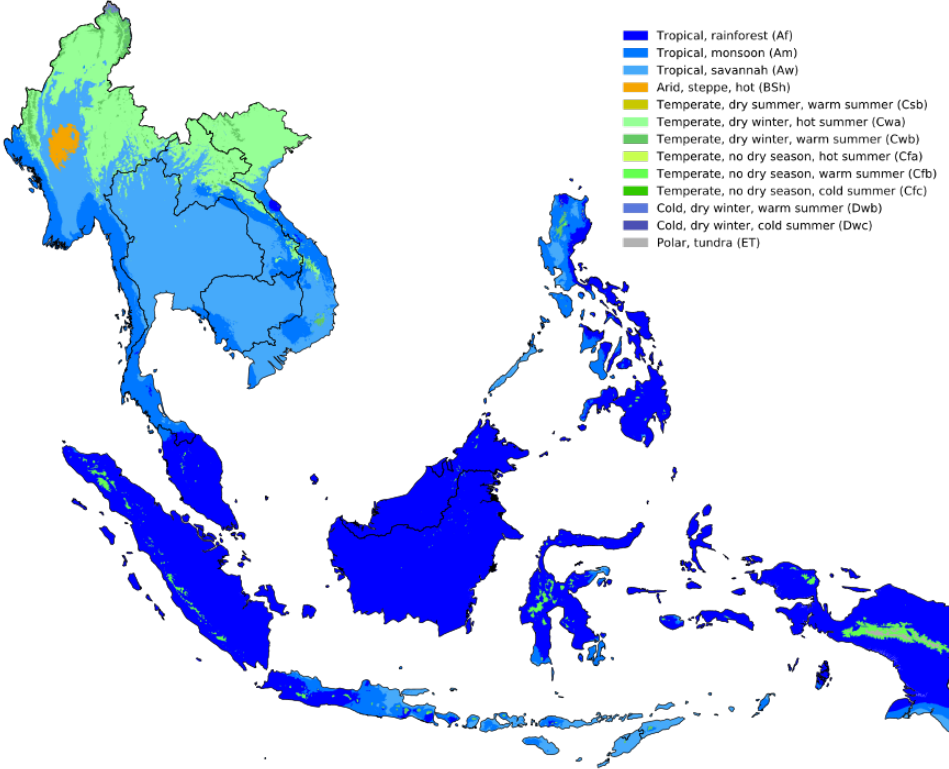


**Figure 1:** Koppen Climate classification of the Maritime Continent according to [Beck et al. \[2018\]](#).

flectivity of the surface

Therefore, in Section 2, I outline the datasets that I used for exploratory analysis and the methods that I used to ensure that the data was viable. In Section 3, I present the results of my comparison between GNSS, MIMIC-TPW2m and ERA5 datasets. In Section 4, I then compare hourly-mean precipitable water against the hourly precipitation rates. I conclude and summarize my results in Section 5.

## Methodology

### Study Area

In my project, the region of study is bounded from 90–165°E and from 15°S to 20°N. Therefore, this region encompasses all of the Southeast Asian countries, including those from the mainland. Although my analysis will be focused on the Maritime Continent which is centered about Indonesia and the Philippines, where relevant I will also contrast the

Maritime Continent with continental Southeast Asia, which includes Myanmar, Thailand and Indochina.

The climatology within my region of study is mostly tropical, except for the northernmost parts of continental Southeast Asia [[Peel et al., 2007](#), [Beck et al., 2018](#)]. The majority of the Maritime Continent is classified as a tropical rainforest (*Af*) climate with relatively uniform precipitation throughout the year, while continental Southeast Asia is mostly classified as tropical savanna (*Aw*) due to extremely dry winters [[Beck et al., 2018](#)]. However, the Koppen-Gieger classification is very general and does not capture many climatological features of the Maritime Continent, such as the predominant role of the diurnal cycle of rainfall that is considered a major characteristic of the region [[Holland and Keenan, 1980](#), [Houze et al., 1981](#), [Johnson and Priegnitz, 1981](#), [Neale and Slingo, 2003](#), [Qian, 2008](#)].

The Maritime Continent is so named because of the dominance of island archipelagos [[Ramage,](#)

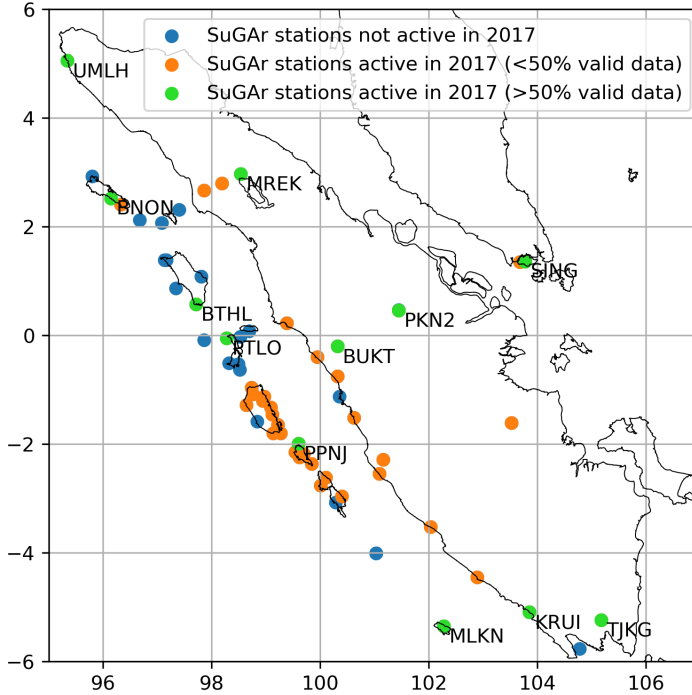


**Figure 2:** Map of Sumatra and the SuGAr stations installed as of present time.

1968]. The predominance of islands and the unique land-sea distribution gives rise to a strong diurnal cycle of convection [Holland and Keenan, 1980, Houze et al., 1981, Johnson and Priegnitz, 1981, Neale and Slingo, 2003, Qian, 2008] that is one of the most active in the world. This diurnal cycle modulates and is modulated by larger-scale atmospheric circulation such as the Madden-Julian Oscillation (MJO) [Madden and Julian, 1994, Zhang, 2005, Rauniyar and Walsh, 2013], and the monsoon [Yamanaka et al., 2018, Chang et al., 2005]. Understanding the dynamics of the Maritime Continent therefore represents a key component of climate research in the near future and beyond, as is evidenced by international efforts such as the Years of the Maritime Continent.

#### Observational Datasets

I used three main observational datasets: (1) Global Precipitation Mission (GPM) IMERG satellite data for precipitation accumulated every 30 minutes [Hou et al., 2014, Huffman et al., 2019], (2) Morphed Integrated Microwave Imagery at CIMSS

(MIMIC)-TPW2m satellite data containing snapshots of precipitable water every hour, and (3) Global Navigation Satellite Systems (GNSS)-derived precipitable water every 10 mins, taken from the Sumatran GPS Array (SuGAr) [Feng et al., 2015]. In order to do intercomparison between datasets, I averaged the GPM precipitation and GNSS-derived precipitable water values into hourly datasets. Data was retrieved for the entire Maritime Continent for 2017 and 2018 for precipitable water, while precipitation data was retrieved from 2001 to 2008. The native resolution of IMERG data is  $0.1^\circ \times 0.1^\circ$ , while that for MIMIC is  $0.25^\circ \times 0.25^\circ$ .

Observational datasets often have missing data, and this is especially true for the GNSS-derived precipitable water data, where stations may not be operational for long periods of time due to damage, or where the data is otherwise deemed to be unreliable due to potentially large errors made in that specific measurement. Therefore, when I average GNSS precipitable water into hourly datasets, I deem an hourly data point as “missing” if there are missing

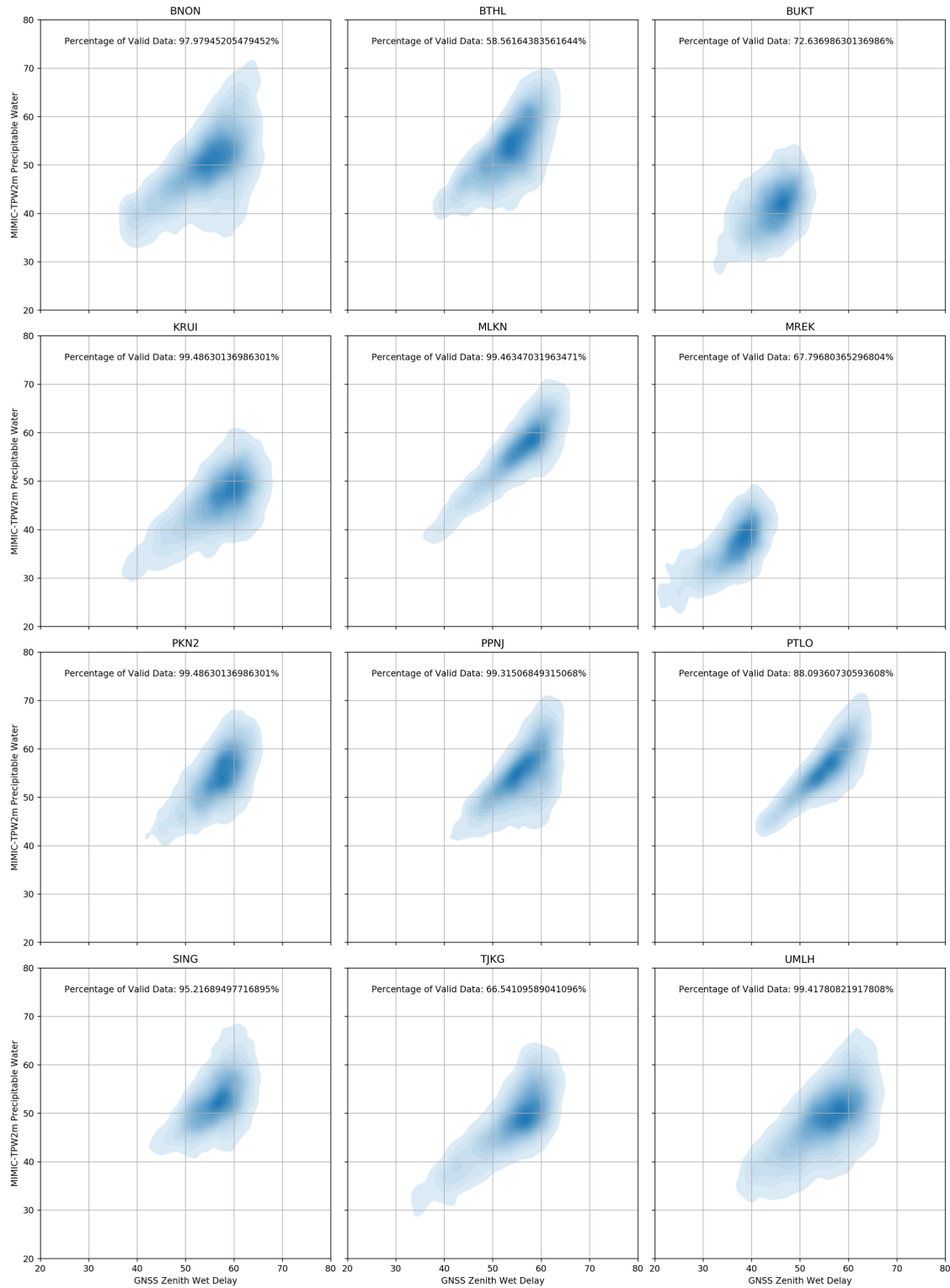


**Figure 3:** Kernel density plots of MIMIC-TPW2m precipitable water against GNSS-derived precipitable water.

data points within the hour. However, I find that from 2017 to 2018, the MIMIC-TPW2m and GPM IMERG datasets have relatively negligible missing data ( $\sim 1$  and 0% for MIMIC-TPW2m and GPM IMERG respectively). Therefore, in my analysis of the climatology of the Maritime Continent using these two datasets I ignore this missing data.

### *Reanalysis Datasets*

The reanalysis datasets used in this project are precipitation and total column water products from the European Centre for Medium-Range Weather Forecasts (ECMWF), ERA-Interim [Dee et al., 2011] and ERA5 [Hersbach and Dee, 2016]. The reanalysis models aim to develop comprehensive records based upon assimilation of various observational data. In the case of the ERA-Interim model, ECMWF aimed to improve the representation of the hydrological cycle, and the handling of various biases in observations. These measures have largely been successful, but representation of the Earth's climate in many aspects, such as the diurnal cycle of rainfall in the Maritime Continent, still require significant improvement. Cloud cover, an important aspect of convection and condensation, remained an unresolved issue [Dee et al., 2011].

ERA5 represents a significant update to ERA-Interim that would allow an easier comparison with the abovementioned datasets due to higher temporal resolution in the model output. ERA-Interim's native resolution is  $0.75^\circ \times 0.75^\circ$ , while that of ERA5 is  $0.25^\circ \times 0.25^\circ$ . ERA-Interim also has a temporal resolution of every 6 hours, while ERA5 increased the frequency of the data output to every hour. Furthermore, ERA5 has many more levels in the vertical, and is able to better represent tropical cyclones, and most importantly, precipitation over land in the deep tropical regions. Therefore, I aim in this project to compare and validate these claims for the Maritime Continent.

### **Validation of Precipitable Water Datasets**

I compared both MIMIC-TPW2m and ERA5 precipitable water datasets against GNSS-derived

precipitable water over the course of 2017. As mentioned in the previous section, since the GNSS-derived precipitable water was taken at steps of every 10 minutes, in order to perform an hourly comparison I need to account for missing data when averaging the GNSS datasets. An hourly data point is deemed as "missing" if there are missing data points within the hour. There are 42 stations in SuGAr for which data are available in 2017 (Fig. 2), though even for these stations there often are missing data within the year as well. I only consider stations for which more than 50% of the data was valid. However, this means that there are only 12 stations which can be used to validate the MIMIC dataset.

### *Conversion of zenith wet delay to precipitable water*

The precision of GNSS technologies relies on my ability to correct for the path difference when the radio frequencies propagate through a medium and are therefore refracted. When these signals pass through the atmosphere, the delay has two components - (1) the ionospheric delay and (2) the tropospheric delay. The ionospheric delay is easily corrected for by broadcasting dual frequencies, as the degree of refraction in the ionosphere is dependent on the frequency of the waves. However, the tropospheric delay is not as easily corrected for, and has both a (a) dry and (b) wet component. The dry component is usually modelled based on surface pressure, and the wet component is dependent on the amount of water along the path, which is then mapped to the zenith direction to produce the zenith wet delay.

The conversion of zenith wet delay to precipitable water has been well studied. [Askne and Nordius \[1987\]](#) were the first to propose a relationship between the two:

$$\text{PWV} = \text{ZWD} \cdot \Pi, \quad \Pi = \frac{10^6}{\rho R_v \left( k'_2 + \frac{k_3}{T_m} \right)} \quad (1)$$

Where  $T_m$  in equation (1) is given by

$$T_m = \frac{\int_0^\infty \frac{e(z)}{T(z)} dz}{\int_0^\infty \frac{e(z)}{T^2(z)} dz} = \frac{\sum_i \frac{e_i}{T_i} \Delta h_i}{\sum_i \frac{e_i}{T_i^2} \Delta h_i}$$

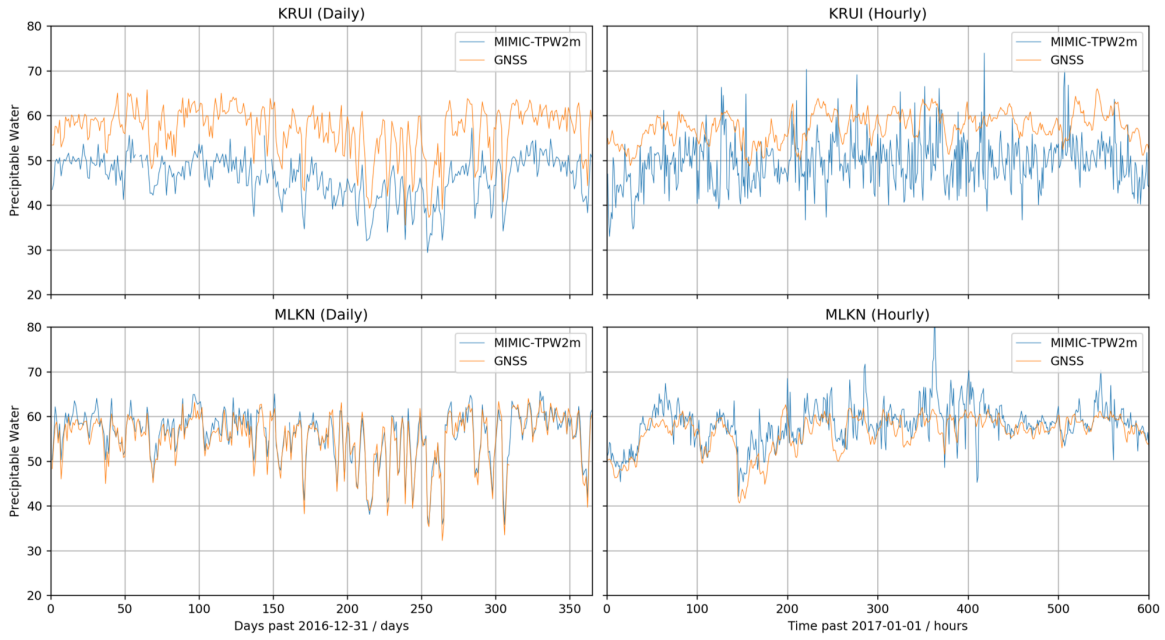


**Figure 4:** Time series plots of GNSS-derived precipitable water and MIMIC-TPW2m precipitable water for (left) daily and (right) hourly data, for the stations (top) KRUI and (bottom) MLKN.

$T_m$  and therefore  $\Pi$  can be taken as constant within the tropics (see Appendix). Therefore, by calculating the global gridded values of  $\Pi$  from ERA-Interim reanalysis data and taking the values of  $\Pi$  nearest to each GNSS station, I am able to derive values of precipitable water from zenith wet delay data for the stations in Fig. 2.

#### Comparing MIMIC-TPW2m to GNSS

The results of my comparison can be seen in Fig. 3. I see that over stations where there is relatively little landmass (MLKN, PPNJ and PTLO), that overall the relationship between the MIMIC-TPW2m and GNSS precipitable water datasets could be said to be more linear in nature (i.e. the regions of high kernel density show a linear trend compared to the outliers). A quick visual time-series comparison of the two datasets against time shows that indeed MIMIC-TPW2m and GNSS have a similar large-scale pattern at daily timescales and above. However, at the hourly timescale, MIMIC-TPW2m shows extremely high variability that may not be accurate. This is likely due to the morphing algorithm used in MIMIC-TPW2m

that has relatively large errors over land compared to the over the ocean.

These results also do indicate that it might be possible to use a moving-average filter to smooth out the variability that I find in the MIMIC-TPW2m data. However, the arbitrary nature of the application of such a filter means that such an investigation is beyond the scope of this project. Therefore, I confine My understanding of the climatology using MIMIC-TPW2m as of now to timescales longer than that of a day. I also note that several stations (KRUI and SING in particular) show systematic dry biases in MIMIC-TPW2m compared to GNSS precipitable water. This is another area of interest that can be studied in the future, though for the purposes of this project we simply note that there is the possibility of systematic bias in MIMIC-TPW2m data even as we use it to try and understand the spatial characteristics of precipitable water over the Maritime Continent.

#### Comparing ERA5 Total Column Water to GNSS

In contrast to MIMIC-TPW2m, the ERA5 total column water dataset has a much more linear rela-

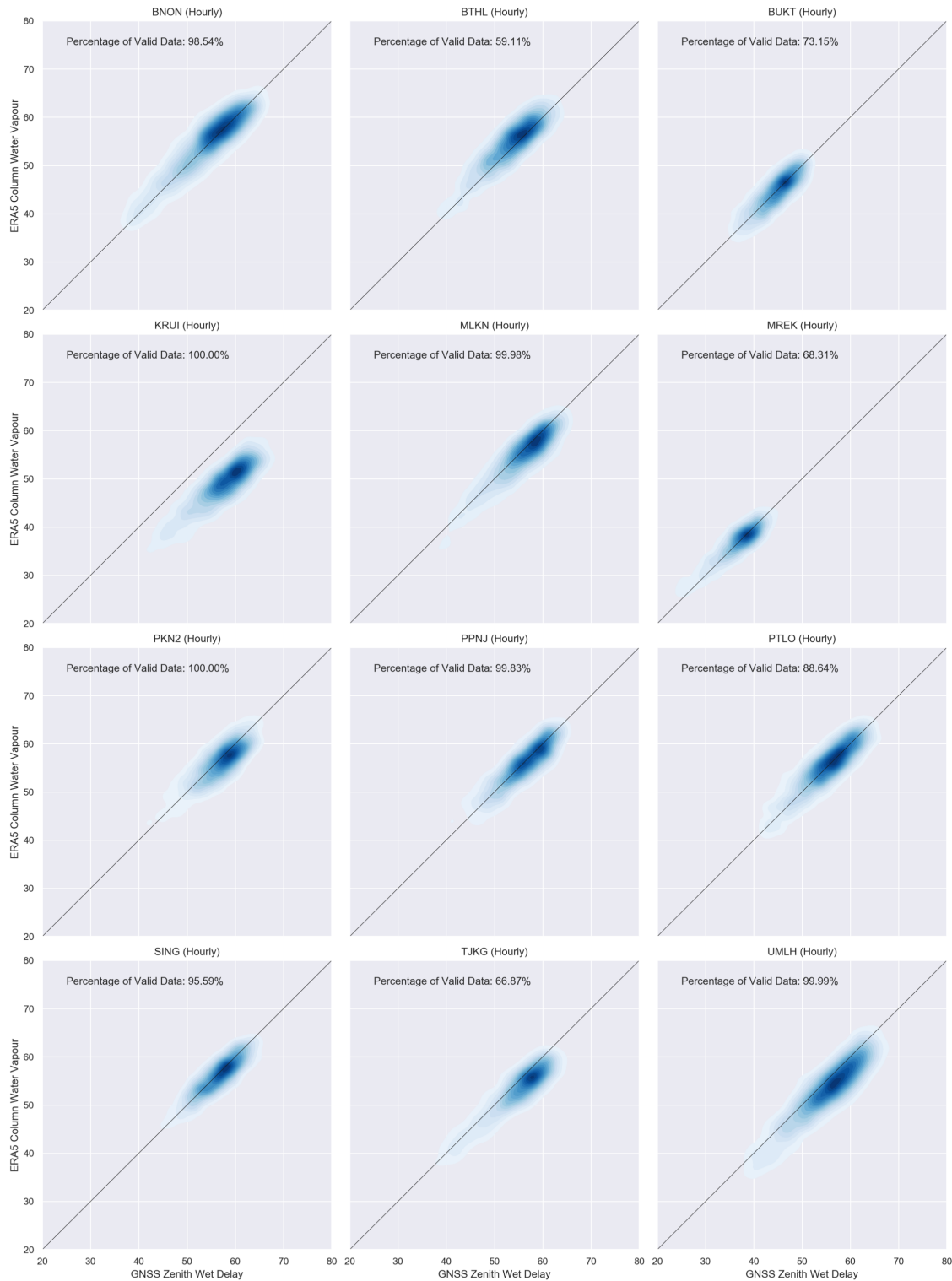


**Figure 5:** Kernel density plots of ERA5 total column water against GNSS-derived precipitable water.



**Figure 6:** Time series plots of GNSS-derived precipitable water and ERA5 total column water for (left) daily and (right) hourly data, for the stations (top) KRUI and (bottom) MLKN.

tionship to GNSS-derived precipitable water regardless of location (Fig. 5). This indicates that ERA5 total column water is more reliable as an estimator of precipitable water than MIMIC-TPW2, if we take the GNSS precipitable water to be the ground truth. As with MIMIC-TPW2m data, we also do a time-series comparison of the two datasets shows once again that at the hourly timescale, ERA5 often shows some lead-lag relationship with GNSS precipitable water data, or may alternatively show less or more variability than GNSS precipitable water. Therefore, ERA5 may not be able to capture the precipitation dynamics and characteristics of the Maritime Continent at the hourly timescale, though this may have to be left for a future investigation. Once again though, at the daily timescale the relationship is shown to be much tighter, with ERA5 column water vapour measurements almost entirely overlapping the GNSS precipitable water values.

We note that by combining the ERA5 and MIMIC-TPW2m datasets, we are occasionally able to show that certain GNSS stations might have a dry or wet bias. This can be seen for the KRUI GNSS

station, which has a consistent wet bias compared to both the MIMIC-TPW2m and ERA5 datasets.

#### *Spatial Comparison of MIMIC-TPW2m to ERA5*

The disadvantage of using GNSS stations is that without high station densities we are unable to characterize the spatial distribution of precipitable water. This is therefore an area where reanalysis and satellite observations hold a critical advantage over GNSS in climate analysis. From the comparison of both ERA5 and MIMIC-TPW2m datasets to GNSS precipitable water, we have concluded that ERA5 likely is the more accurate of the two if we were to take the GNSS precipitable water values as ground truth. Since out of the 12 stations where data was available in 2017, 4 (MREK, PKN2, BUKT and TJKG) were located as a significant distance inland, we believe that the above analysis also shows that the accuracy of ERA5 column water vapour data is not dependent on the distance inland.

Taking advantage of the fact that the ERA5 analysis has a relatively high correlation to the GNSS stations with enough valid data, which we assume in this

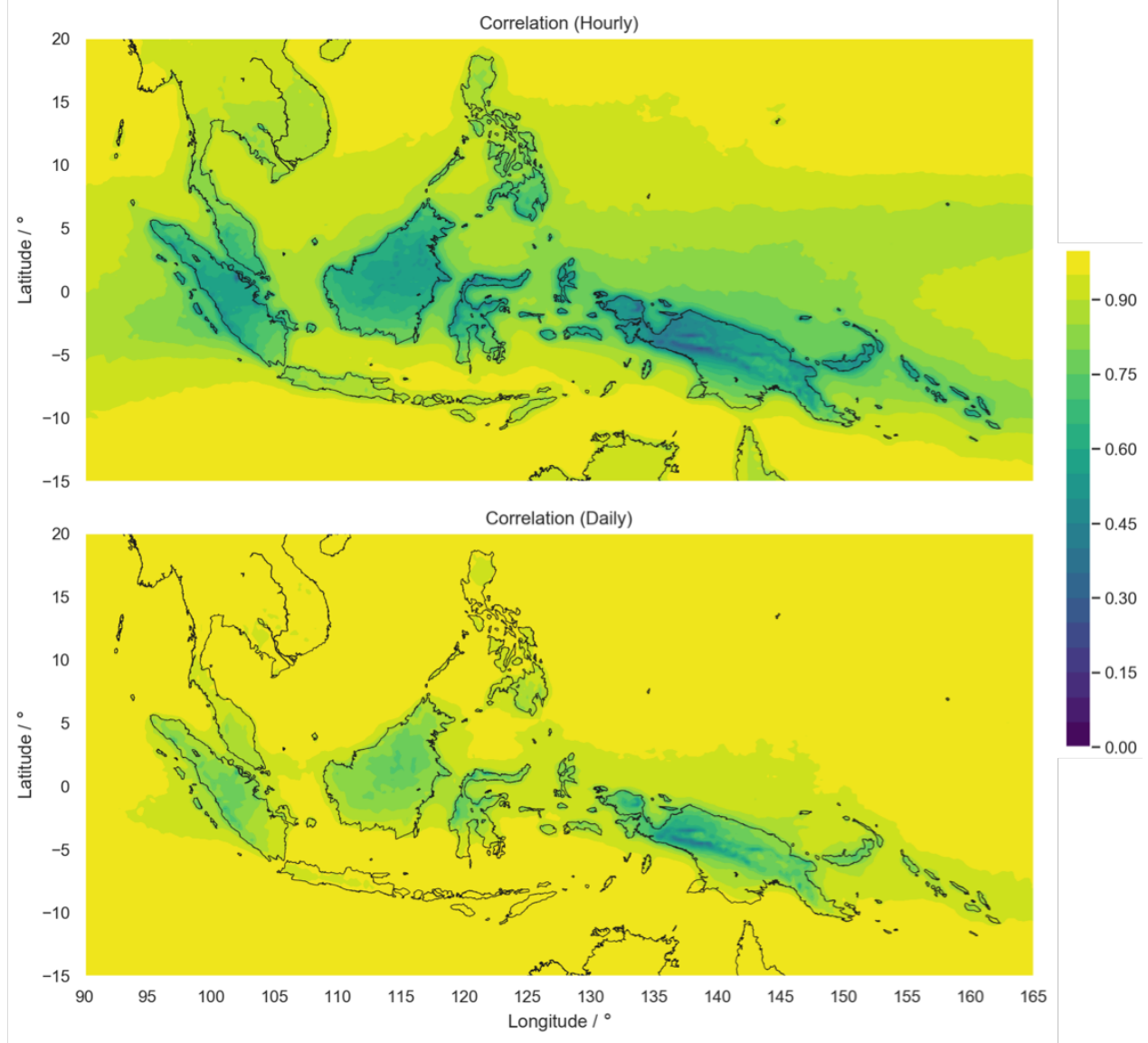


**Figure 7:** Contour plot of the spatial correlation of ERA5 total column water against MIMIC-TPW2m precipitable water for (top) hourly and (bottom) daily data.

project to be the ground truth, and also that ERA5 reanalysis allows for gridded global coverage, we then proceed to determine where the MIMIC-TPW2m algorithm for retrieval of precipitable water performs better, for both hourly and daily data, by performing correlation for each every grid point for precipitable water data over 2017 and 2018. (*Note: this was made easy because both ERA5 and MIMIC-TPW2m both have native  $0.25^\circ \times 0.25^\circ$  spatial resolution*).

We see from Fig. 7 that, as expected, the performance of the MIMIC-TPW2m algorithm decreases significantly near land, particularly near regions of high and complex topography, such as in Papua New Guinea, and to a lesser extent Sumatra and Borneo, where regions of high topography can be seen. But it must be noted that this is not a linear relation, and from Fig. 8 it can be seen that there seem to be two distinct regimes at play within the Maritime

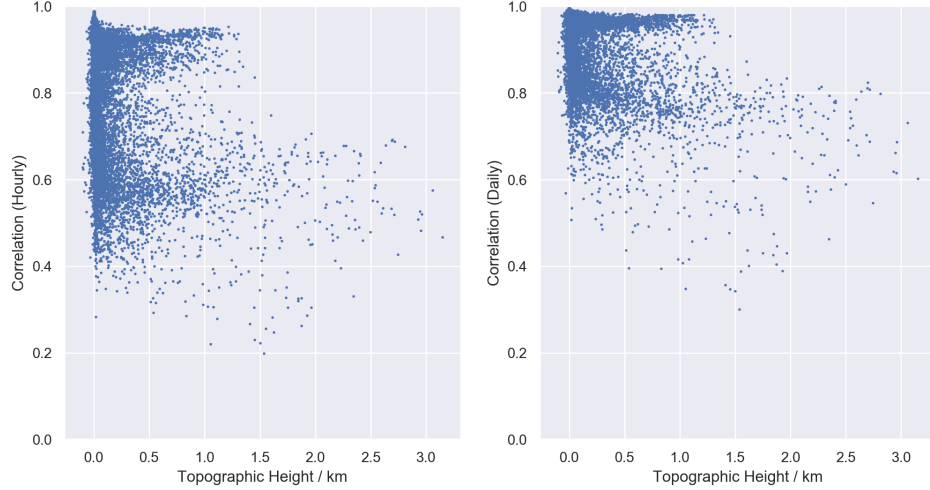


**Figure 8:** Scatter plots showing the relationship between the correlation of ERA5 total column water and MIMIC-TPW2m precipitable water, against orographic height in km.

Continent that determines how accurate the MIMIC-TPW2m algorithm is at retrieving precipitable water.

We note that for hourly data that over the oceans, correlation tends to be noticeably lower simply within the tropical regions itself, though proximity to land also undoubtedly plays a role. In the hourly data, we notice at the eastern boundary of our region that there is a region of slightly lower correlation extending to the east at around  $5^{\circ}\text{N}$  parallel to the equator, and another tail moving southeast off the coast of Papua New Guinea. This is possibly analogous to the double-ITCZ phenomenon, and could indicate that the presence of clouds along the ITCZ could affect the accuracy of the precipitable water retrieval algorithms for MIMIC-TPW2m. However, more work needs to be done to confirm this hypothesis.

### Comparing Precipitation and Precipitable Water

In this section, we compare GPM precipitation against ERA5 precipitable water. Previous studies [Peters and Neelin, 2006, Neelin et al., 2009, Muller et al., 2009] using precipitable water measurements over the ocean have shown that precipitation increases with water vapour, and at some critical boundary  $w$ , the averaged-rate of precipitation increases sharply. However, these studies focus on precipitable water measurements over the ocean due to

limitations of microwave sensing over land. Therefore, using improved representation of precipitable water in the ERA5 reanalysis model, we aim to determine if this relationship also holds over land as well. Over the region of study, we extracted the hourly-averaged GPM precipitation rain rate, and found the average precipitation for precipitable water values binned every 0.5 mm from 10 mm to 80 mm. We also differentiated our results against land and sea.

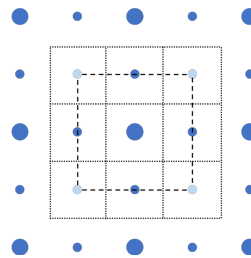


**Figure 9:** Diagram illustrating the sampling of data. Large points indicate where full weightage is taken, small points indicate where the weightage is 0.5, and light-coloured points indicate weightage of 0.25. This is based off the area of the initial grid (dotted lines) that intersect with the new grid (dashed lines).

To save time, the horizontal resolution was lowered to  $0.5^{\circ}$ . Thus, we also readjusted the land-sea mask from ERA5 to every  $0.5^{\circ}$  as well. In ERA5,

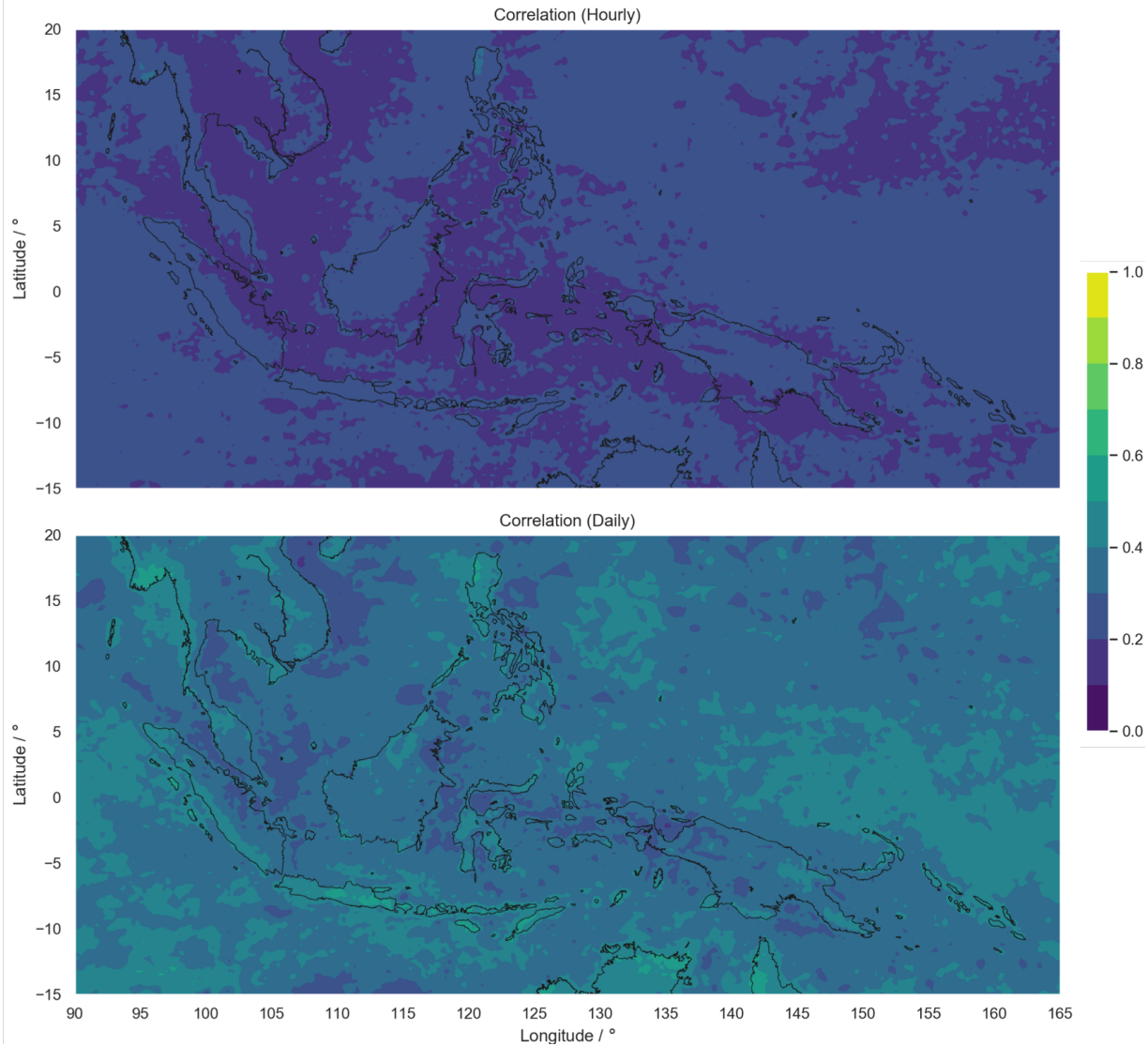


**Figure 10:** The spatial correlation of ERA5 total column water against GPM precipitation rate for (top) hourly and (bottom) daily data.

land points are given a value of 1 while all other points are given a value of zero. We sum the points in the new grid, weighting the points based on the degree to which their grids intersect the new grid (see Fig. 9). If the weighted sum is greater than 0.5, then we consider the grid to be a land-point, and ocean otherwise.

We first plotted the spatial correlation of time-series ERA5 precipitable water against GPM precipitation (Fig. 10). We see that attempting to di-

rectly correlate the two variables does not yield any meaningful results or relationship at either the hourly or daily timescales. Therefore, we directly proceed to finding the mean precipitation intensity for each binned value of ERA5 precipitable water (Fig. 11), for all points, as well as distinguishing between land points and sea. By plotting for each precipitable water bin the ratio of the frequency at which values within the bin occur over land as compared to the ocean, we see that extremely high values of precip-

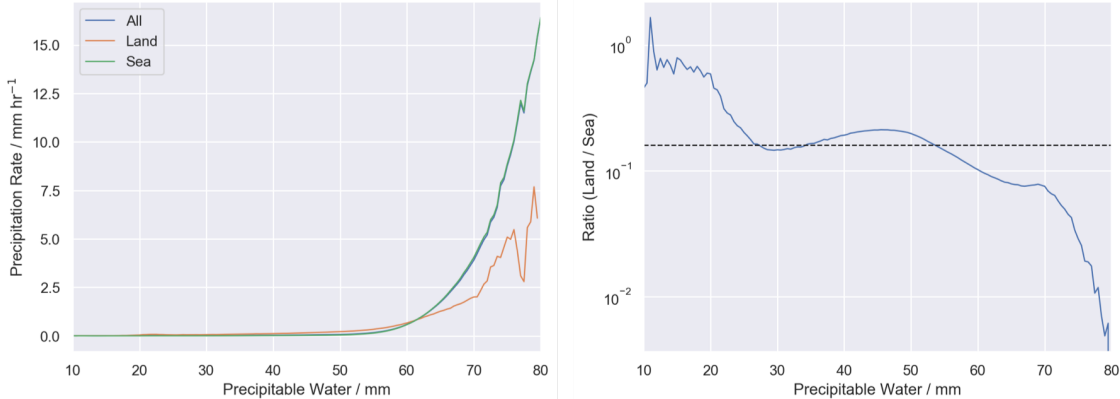


**Figure 11:** Plot of (left) bin-averaged GPM precipitation rate against ERA5 total column water, and (right) the ratio of the frequency of precipitable water values found over land compared to over the ocean, with the dashed black line representing the ratio of the number of land points to ocean points.

itable water tend to occur over the ocean, while the reverse is true over land.

Because of the predominance of ocean points compared to land points, we see that there is relatively little difference in the domain-averaged precipitation rate distribution compared to that over only ocean. By separating out the points over land, we note that there is a much lower precipitation rate over land as compared to over the ocean, and this is especially obvious when precipitable water is high. However, it is entirely possible that this is a result of undersampling, as values of precipitable water that are this high rarely occur over land.

We note that our curve is slightly different from that given by Peters and Neelin [2006]. In our diagram, we do see that precipitation rate begins to increase sharply at around total column water vapour of 65 mm depth. However, unlike Peters and Neelin [2006], we see that this increase seems to resemble an exponential curve, as opposed to there being a true “critical point” of precipitable water where precipitation rate jumps sharply and then increases more gradually. The reason behind this is as of yet uncertain, and should be investigated further.

## Conclusion

In this project, we have investigated satellite and reanalysis products for precipitation and precipitable

water. We show, through comparison with GNSS-derived precipitable water, that satellite-based products for precipitable water such as MIMIC-TPW2m overestimate the variability of precipitable water over land compared to reanalysis data. Therefore, we believe that ERA5 currently holds more promise in allowing us to investigate precipitable water over the Maritime Continent compared to satellite data.

Through comparison of ERA5 precipitable water with GPM-derived precipitation rates, we attempt to recreate the relationship established by Peters and Neelin [2006] between tropical precipitable water and precipitation rates. However, we find that, either due to a undersampling of data or other errors involved, there is no obvious “critical point” at which precipitation rate drastically increases. Instead, when using reanalysis data we find that precipitation rate is likely an exponential function of precipitable water. More testing needs to be done over a longer period of time to verify this trend, because there are very little data when precipitable water values of at the higher extremes, especially over land.

## Addendum

All codes used for analysis in this project are available on my Github: [https://github.com/natgeo-wong/Isca\\_prj](https://github.com/natgeo-wong/Isca_prj). The data were downloaded using ClimateSatellite.jl, ClimateERA.jl, ClimateG-

NSS.jl. Scripts that make use of the downloaded data are mostly found in ClimateScripts.jl.

## References

- J. Askne and H. Nordius. Estimation of tropospheric delay for microwaves from surface weather data. *Radio Science*, 22(3):379–386, 5 1987. ISSN 00486604. doi: 10.1029/RS022i003p00379. URL <http://doi.wiley.com/10.1029/RS022i003p00379>.
- H. E. Beck, N. E. Zimmermann, T. R. McVicar, N. Vergopolan, A. Berg, and E. F. Wood. Present and future Köppen-Geiger climate classification maps at 1-km resolution. *Scientific Data*, 5 (1):180214, 12 2018. ISSN 2052-4463. doi: 10.1038/sdata.2018.214. URL <http://www.nature.com/articles/sdata2018214>.
- C.-P. Chang, Z. Wang, J. McBride, and C.-H. Liu. Annual Cycle of Southeast AsiaMaritime Continent Rainfall and the Asymmetric Monsoon Transition. *Journal of Climate*, 18(2):287–301, 1 2005. ISSN 0894-8755. doi: 10.1175/JCLI-3257.1. URL <http://journals.ametsoc.org/doi/abs/10.1175/JCLI-3257.1>.
- D. P. Dee, S. M. Uppala, A. J. Simmons, P. Berrisford, P. Poli, S. Kobayashi, U. Andrae, M. A. Balmaseda, G. Balsamo, P. Bauer, P. Bechtold, A. C. M. Beljaars, L. van de Berg, J. Bidlot, N. Bormann, C. Delsol, R. Dragani, M. Fuentes, A. J. Geer, L. Haimberger, S. B. Healy, H. Hersbach, E. V. Hólm, L. Isaksen, P. Kållberg, M. Köhler, M. Matricardi, A. P. McNally, B. M. Monge-Sanz, J.-J. Morcrette, B.-K. Park, C. Peubey, P. de Rosnay, C. Tavolato, J.-N. Thépaut, and F. Vitart. The ERA-Interim reanalysis: configuration and performance of the data assimilation system. *Quarterly Journal of the Royal Meteorological Society*, 137(656):553–597, 4 2011. ISSN 00359009. doi: 10.1002/qj.828. URL <http://doi.wiley.com/10.1002/qj.828>.
- L. Feng, E. M. Hill, P. Banerjee, I. Hermawan, L. L. H. Tsang, D. H. Natawidjaja, B. W. Suwarsono, and K. Sieh. A unified GPS-based earthquake catalog for the Sumatran plate boundary between 2002 and 2013. *Journal of Geophysical Research: Solid Earth*, 120(5):3566–3598, 5 2015. ISSN 21699313. doi: 10.1002/2014JB011661. URL <http://doi.wiley.com/10.1002/2014JB011661>.
- H. Hersbach and D. Dee. ERA5 reanalysis is in production. *ECMWF Newsletter*, (147):7, 2016. URL <https://confluence.ecmwf.int/pages/viewpage.action?pageId=74764925>.
- G. J. Holland and T. D. Keenan. Diurnal Variations of Convection over the Maritime Continent. *Monthly Weather Review*, 108(2):223–225, 2 1980. ISSN 0027-0644. doi: 10.1175/1520-0493(1980)108<0223:DVCOT>2.0.CO;2. URL <http://journals.ametsoc.org/doi/abs/10.1175/1520-0493%281980%29108%3C0223%3ADVOCOT%3E2.0.CO%3B2>.
- A. Y. Hou, R. K. Kakar, S. Neeck, A. A. Azbarzin, C. D. Kummerow, M. Kojima, R. Oki, K. Nakamura, and T. Iguchi. The Global Precipitation Measurement Mission. *Bulletin of the American Meteorological Society*, 95(5):701–722, 5 2014. ISSN 0003-0007. doi: 10.1175/BAMS-D-13-00164.1. URL <http://journals.ametsoc.org/doi/abs/10.1175/BAMS-D-13-00164.1>.
- R. A. Houze, S. G. Geotis, F. D. Marks, and A. K. West. Winter Monsoon Convection in the Vicinity of North Borneo. Part I: Structure and Time Variation of the Clouds and Precipitation. *Monthly Weather Review*, 109(8):1595–1614, 8 1981. ISSN 0027-0644. doi: 10.1175/1520-0493(1981)109<1595:WMCITV>2.0.CO;2. URL <http://journals.ametsoc.org/doi/abs/10.1175/1520-0493%281981%29109%3C1595%3AWMCITV%3E2.0.CO%3B2>.
- G. Huffman, E. Stocker, D. Bolvin, E. Nelkin, and J. Tan. GPM IMERG Final Precipitation L3 Half Hourly 0.1 degree x 0.1 degree V06, 2019.

- P. M. Inness and J. M. Slingo. The interaction of the Madden-Julian Oscillation with the Maritime Continent in a GCM. *Quarterly Journal of the Royal Meteorological Society*, 132(618):1645–1667, 7 2006. ISSN 00359009. doi: 10.1256/qj.05.102. URL <http://doi.wiley.com/10.1256/qj.05.102>.
- R. H. Johnson and D. L. Priegnitz. Winter Monsoon Convection in the Vicinity of North Borneo. Part II: Effects on Large-Scale Fields. *Monthly Weather Review*, 109(8): 1615–1628, 8 1981. ISSN 0027-0644. doi: 10.1175/1520-0493(1981)109<1615:WMCITV>2.0.CO;2. URL <http://journals.ametsoc.org/doi/abs/10.1175/1520-0493%281981%29122%3C0814%3AOOTDTO%3E2.0.CO%3B2>.
- N. C. Jourdain, A. S. Gupta, A. S. Taschetto, C. C. Ummenhofer, A. F. Moise, and K. Ashok. The Indo-Australian monsoon and its relationship to ENSO and IOD in reanalysis data and the CMIP3/CMIP5 simulations. *Climate Dynamics*, 41(11-12):3073–3102, 12 2013. ISSN 0930-7575. doi: 10.1007/s00382-013-1676-1. URL <http://link.springer.com/10.1007/s00382-013-1676-1>.
- J. Ling, C. Zhang, R. Joyce, P. Xie, and G. Chen. Possible Role of the Diurnal Cycle in Land Convection in the Barrier Effect on the MJO by the Maritime Continent. *Geophysical Research Letters*, 46(5):3001–3011, 3 2019a. ISSN 0094-8276. doi: 10.1029/2019GL081962. URL <https://onlinelibrary.wiley.com/doi/abs/10.1029/2019GL081962>.
- J. Ling, Y. Zhao, and G. Chen. Barrier Effect on MJO Propagation by the Maritime Continent in the MJO Task Force/GEWEX Atmospheric System Study Models. *Journal of Climate*, 32(17): 5529–5547, 9 2019b. ISSN 0894-8755. doi: 10.1175/JCLI-D-18-0870.1. URL <http://journals.ametsoc.org/doi/10.1175/JCLI-D-18-0870.1>.
- B. S. Love, A. J. Matthews, and G. M. S. Lister. The diurnal cycle of precipitation over the Maritime Continent in a high-resolution atmospheric model. *Quarterly Journal of the Royal Meteorological Society*, 137(657):934–947, 4 2011. ISSN 00359009. doi: 10.1002/qj.809. URL <http://doi.wiley.com/10.1002/qj.809>.
- R. A. Madden and P. R. Julian. Observations of the 4050-Day Tropical OscillationA Review. *Monthly Weather Review*, 122(5):814–837, 5 1994. ISSN 0027-0644. doi: 10.1175/1520-0493(1994)122<0814:OOTDTO>2.0.CO;2. URL <http://journals.ametsoc.org/doi/abs/10.1175/1520-0493%281994%29122%3C0814%3AOOTDTO%3E2.0.CO%3B2>.
- C. J. Muller, L. E. Back, P. A. O’Gorman, and K. A. Emanuel. A model for the relationship between tropical precipitation and column water vapor. *Geophysical Research Letters*, 36(16): L16804, 8 2009. ISSN 0094-8276. doi: 10.1029/2009GL039667. URL <http://doi.wiley.com/10.1029/2009GL039667>.
- R. Neale and J. Slingo. The Maritime Continent and Its Role in the Global Climate: A GCM Study. *Journal of Climate*, 16(5):834–848, 3 2003. ISSN 0894-8755. doi: 10.1175/1520-0442(2003)016<0834:TMCAIR>2.0.CO;2. URL <http://journals.ametsoc.org/doi/abs/10.1175/1520-0442%282003%29016%3C0834%3ATMCAIR%3E2.0.CO%3B2>.
- J. D. Neelin, O. Peters, and K. Hales. The Transition to Strong Convection. *Journal of the Atmospheric Sciences*, 66(8):2367–2384, 8 2009. ISSN 0022-4928. doi: 10.1175/2009JAS2962.1. URL <http://journals.ametsoc.org/doi/abs/10.1175/2009JAS2962.1>.
- M. C. Peel, B. L. Finlayson, and T. A. McMahon. Updated world map of the Köppen-Geiger climate classification. *Hydrology and Earth System Sciences*, 11(5):1633–1644, 10 2007. ISSN 1607-7938. doi: 10.5194/hess-11-1633-2007. URL <http://www.hydrol-earth-syst-sci.net/11/1633/2007/>.

- O. Peters and J. D. Neelin. Critical phenomena in atmospheric precipitation. *Nature Physics*, 2(6):393–396, 6 2006. ISSN 1745-2473. doi: 10.1038/nphys314. URL <http://www.nature.com/articles/nphys314>.
- J.-H. Qian. Why Precipitation Is Mostly Concentrated over Islands in the Maritime Continent. *Journal of the Atmospheric Sciences*, 65(4):1428–1441, 4 2008. ISSN 0022-4928. doi: 10.1175/2007JAS2422.1. URL <http://journals.ametsoc.org/doi/abs/10.1175/2007JAS2422.1>.
- C. S. Ramage. Role of a Tropical "Maritime Continent" in the Atmospheric Circulation. *Monthly Weather Review*, 96(6):365–370, 6 1968. ISSN 0027-0644. doi: 10.1175/1520-0493(1968)096<0365:ROATMC>2.0.CO;2. URL <http://journals.ametsoc.org/doi/abs/10.1175/1520-0493%281968%29096%3C0365%3AROATMC%3E2.0.CO%3B2>.
- S. P. Rauniyar and K. J. E. Walsh. Influence of ENSO on the Diurnal Cycle of Rainfall over the Maritime Continent and Australia. *Journal of Climate*, 26(4):1304–1321, 2 2013. ISSN 0894-8755. doi: 10.1175/JCLI-D-12-00124.1. URL <http://journals.ametsoc.org/doi/abs/10.1175/JCLI-D-12-00124.1>.
- H. Rui and B. Wang. Development Characteristics and Dynamic Structure of Tropical Intraseasonal Convection Anomalies. *Journal of the Atmospheric Sciences*, 47(3):357–379, 2 1990. ISSN 0022-4928. doi: 10.1175/1520-0469(1990)047<0357:DCADSO>2.0.CO;2. URL <http://journals.ametsoc.org/doi/abs/10.1175/1520-0469%281990%29047%3C0357%3ADCADSO%3E2.0.CO%3B2>.
- C. Wang, L. Zhang, S.-K. Lee, L. Wu, and C. R. Mechoso. A global perspective on CMIP5 climate model biases. *Nature Climate Change*, 4(3):201–205, 3 2014. ISSN 1758-678X. doi: 10.1038/nclimate2118. URL <http://www.nature.com/articles/nclimate2118>.
- S. Wang and A. H. Sobel. Factors Controlling Rain on Small Tropical Islands: Diurnal Cycle, Large-Scale Wind Speed, and Topography. *Journal of the Atmospheric Sciences*, 74(11):3515–3532, 11 2017. ISSN 0022-4928. doi: 10.1175/JAS-D-16-0344.1. URL <http://journals.ametsoc.org/doi/10.1175/JAS-D-16-0344.1>.
- C.-H. Wu and H.-H. Hsu. Topographic Influence on the MJO in the Maritime Continent. *Journal of Climate*, 22(20):5433–5448, 10 2009. ISSN 0894-8755. doi: 10.1175/2009JCLI2825.1. URL <http://journals.ametsoc.org/doi/10.1175/2009JCLI2825.1>.
- M. D. Yamanaka. Physical climatology of Indonesian maritime continent: An outline to comprehend observational studies. *Atmospheric Research*, 178-179:231–259, 9 2016. ISSN 01698095. doi: 10.1016/j.atmosres.2016.03.017. URL <http://dx.doi.org/10.1016/j.atmosres.2016.03.017> <https://linkinghub.elsevier.com/retrieve/pii/S0169809516300679>.
- M. D. Yamanaka, S.-Y. Ogino, P.-M. Wu, H. Jun-Ichi, S. Mori, J. Matsumoto, and F. Syamsudin. Maritime continent coastlines controlling Earth's climate. *Progress in Earth and Planetary Science*, 5(1):21, 12 2018. ISSN 2197-4284. doi: 10.1186/s40645-018-0174-9. URL <https://progearthplanetsci.springeropen.com/articles/10.1186/s40645-018-0174-9>.
- C. Zhang. Madden-Julian Oscillation. *Reviews of Geophysics*, 43(2):RG2003, 2005. ISSN 8755-1209. doi: 10.1029/2004RG000158. URL [http://140.90.101.29/products/precip/CWlink/MJO/MJO\\_1page\\_factsheet.pdf](http://140.90.101.29/products/precip/CWlink/MJO/MJO_1page_factsheet.pdf) <http://doi.wiley.com/10.1029/2004RG000158>.